

What value high level concepts in vision to language problems?

Qi Wu, Chunhua Shen, Anton van den Hengel, Lingqiao Liu, Anthony Dick
The University of Adelaide, Adelaide, SA 5005, Australia
e-mail: `firstname.lastname@adelaide.edu.au`

Abstract

Much of the recent progress in Vision-to-Language (*V2L*) problems has been achieved through a combination of Convolutional Neural Networks (CNNs) and Recurrent Neural Networks (RNNs). This approach does not explicitly represent high-level semantic concepts, but rather seeks to progress directly from image features to text. We propose here a method of incorporating high-level concepts into the very successful CNN-RNN approach, and show that it achieves a significant improvement on the state-of-the-art performance in both image captioning and visual question answering. We also show that the same mechanism can be used to introduce external semantic information and that doing so further improves performance. In doing so we provide an analysis of the value of high level semantic information in *V2L* problems.

Contents

1	Introduction	2
2	Related Work	2
3	The Attribute-based <i>V2L</i> Model	4
3.1	Attribute Predictor	5
3.2	Language Generator	6
4	Image Captioning	8
4.1	Dataset	8
4.2	Evaluation	8
5	Visual Question Answering	11
5.1	Dataset	11
5.2	Evaluation	11
5.3	Attributes Expansion using WordNet	12
6	Conclusion	14

arXiv:1506.01144v4 [cs.CV] 9 Oct 2015

1 Introduction

Vision-to-Language problems represent a particular challenge within Computer Vision because they require an element of translation between two different forms of information. This challenge is more acute than that faced in machine translation between languages, because the two forms of information (images and text) are so different. In language translation both languages are human-devised methods of communication, and the content of the original and translated pieces of prose is the same, irrespective of the language. In machine language translation there have been a series of results showing that good performance can be achieved without developing a higher-level model of the state of the world. In [4, 10, 55], for instance, a source sentence is transformed into a fixed-length vector representation by an ‘encoder’ RNN, which in turn is used as the initial hidden state of a ‘decoder’ RNN that generates the target sentence.

Despite the supposed equivalence between an image and 1000 words, the manner in which information is represented in each data form could hardly be more different. Human language is designed specifically so as to communicate information to humans, whereas even the most carefully composed image represents the culmination of a complex set of physical processes over which humans have little control. Given the differences between these two forms of information, it seems surprising that methods which translate directly from image features to text represent the current state of the art in key Vision-to-Language (V2L) problems, such as image captioning and visual question answering. This approach underpins many recent successful works on image captioning, however, such as [9, 12, 26, 43, 58]. All use a CNN as an image ‘encoder’ to produce a fixed-length vector representation [28, 34, 52, 56], which is then fed into the ‘decoder’ RNN to generate a caption.

Visual Question Answering (VQA) is a more recent challenge than image captioning. In this V2L problem an image and a free-form, open-ended question about the image are presented to the method which is required to produce an answer as the output [2]. As in image captioning, the current state of the art in VQA [16, 50] relies on passing CNN features to an RNN language model.

This is a discussion paper and our main contribution is to discuss a fundamental question: *is it really beneficial to bypass the image-to-words mappings in V2L tasks?* We investigate particularly whether adding the capacity to represent high-level information into the CNN-RNN framework improves performance. We do this by adding an explicit representation of attributes of the scene which are meaningful to humans. Each semantic attribute corresponds to a word mined from the training image descriptions, and represents higher-level knowledge about the content of the image. A CNN-based classifier is trained for each attribute, and the set of attribute likelihoods for an image form a high-level representation of image content. An RNN is then trained to generate the required captions, or question answers, on the basis of the likelihoods.

Our technical contribution is to provide a fully trainable attribute based neural network that can be applied to multiple *V2L* problems and which yields significantly better performance than the current state-of-the-art approaches; for example, on the official Microsoft COCO benchmarks, we produced a BLEU-1 score of 0.73 on the image captioning, which is the top 1 on the leaderboard at the time of written this paper. On the visual question answering task, our system yielded a WUPS@0.9 score of 71.15, compared to the current state-of-the-art of 65.36, on the COCO-QA single word question answering dataset. On COCO-VQA, an open-answer task dataset, our method achieves 51.60% accuracy, while the baseline is 27.13% and human performance reaches 61.58%. Moreover, with an expansion from image-sourced attributes to knowledge-sourced through WordNet (see Section 5.3), we further push the accuracy to 53.59%, which is the best reported results so far.

2 Related Work

Attribute-based Representation Using attribute-based models as a high-level representation has shown potential in many computer vision tasks such as object recognition, image annotation and image retrieval. Farhadi *et al.* [14] were among the first to propose to use a set of visual semantic attributes to identify familiar objects, and to describe unfamiliar objects. Lampert *et al.* [32, 33] showed that semantic attributes can be used to recognize object classes in the absence of training images, known as zero-shot learning. In addition to describing objects semantically, there are several works describing the whole image using semantic features. Vogel and Schiele [59] used visual attributes describing scenes to characterize image regions and combined these local semantics into a global image description. Su *et al.* [54] defined six groups of attributes

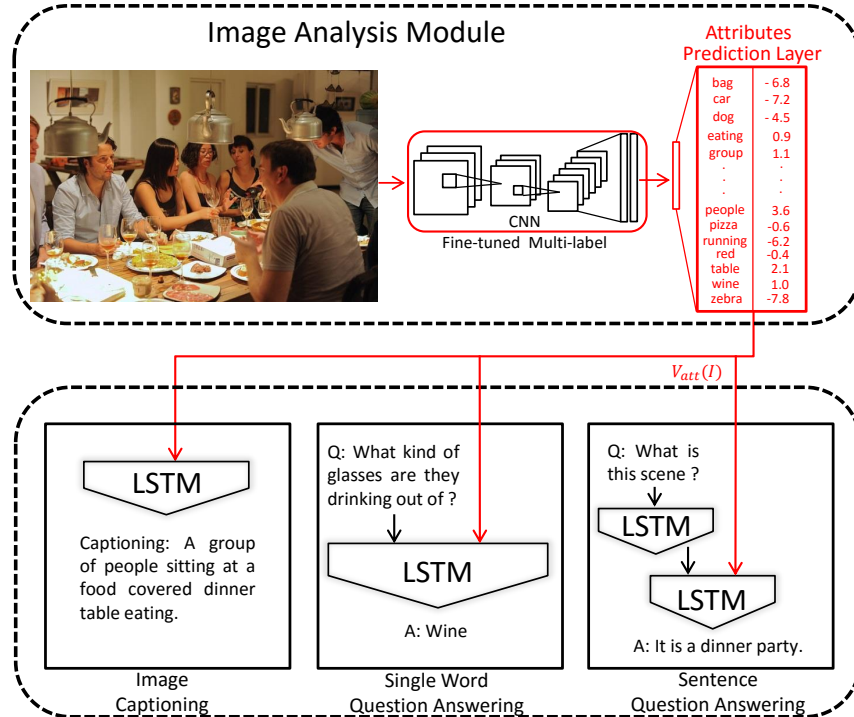


Figure 1 – Our attribute based $V2L$ framework. The image analysis module learns a mapping between an image and the semantic attributes through a CNN. The language module learns a mapping from the attributes vector (the red arrow) to a sequence of words using an LSTM.

to build intermediate level features for image classification. Li *et al.* [35, 36] introduced the concept of an ‘object bank’ which enables objects to be used as attributes for scene representation.

Image Captioning The problem of annotating images with natural language at the scene level has long been studied in both computer vision and natural language processing. Hodosh *et al.* [20] proposed to frame sentence-based image annotation as the task of ranking a given pool of captions. Similarly [18, 22, 47] treat the task as a retrieval problem, but based instead on co-embedding of images and text in the same vector space. Recently, Socher *et al.* [53] used neural networks to co-embed image and sentences together and Karpathy *et al.* [26] co-embedded image crops and sub-sentences. Neither attempted to generate novel captions.

Attributes have been used in many image captioning methods to fill the gaps in predetermined caption templates. Farhadi *et al.* [15], for instance, used detections to infer a triplet of scene elements which is converted to text using a template. Li *et al.* [37] composed image descriptions given computer vision based inputs such as detected objects, modifiers and locations using web-scale n-grams. A more complicated CRF-based use of attribute detections beyond triplets was proposed by Kulkarni *et al* [29]. The advantage of template-based methods is that the resulting captions are more likely to be grammatically correct. The drawback is that they still rely on hard-coded visual concepts and suffer the implied limits on the variety of the output. Instead of using fixed templates, more powerful language models based on language parsing have been developed such as [1, 30, 31, 46].

Fang *et al.* [13] won the 2015 COCO Captioning Challenge with an approach that is similar to ours in as much as it applies a visual concept (i.e. attributes) detection process before generating sentences. They first learned 1000 independent detectors for visual words based on a multi-instance learning framework and then used a maximum entropy language model conditioned on the set of visually detected words directly to generate captions. Although an image-to-word mapping is used in this approach, the sentence generation process is quite restrictive since the words must be drawn from the visual concept alphabet. Instead, we build our attribute alphabet and word vocabulary separately. Our visual attributes act as a high-level

semantic representation for image content which is fed into an LSTM which generates target sentences based on a much larger words vocabulary. In contrast to the Fang *et al.* [13] approach this allows far greater variety and generality in the generated text. In practice, we produced better captioning results than [13] only using a rather small attribute alphabet (size 256) but with a much larger vocabulary (almost 10K). It is impractical for [13] to extend their word vocabulary to a such size as it would require 10K independent attribute detectors. Moreover, the success of their model relies on a re-scoring process from a joint image-text embedding space. To what extent the image-to-word mapping helps in image captioning is not discussed in their work. This is the main focus of this paper.

In contrast to the aforementioned two-stage methods, the recent dominant trend in *V2L* is to use an architecture which connects a CNN to an RNN to learn the mapping from images to sentences directly. Mao *et al.* [43], for instance, proposed a multimodal RNN (m-RNN) to estimate the probability distribution of the next word given previous words and the deep CNN feature of an image at each time step. Similarly, Kiros *et al.* [27] constructed a joint multimodal embedding space using a powerful deep CNN model and an LSTM that encodes text. Karpathy and Li [25] also proposed a multimodal RNN generative model, but in contrast to [43], their RNN is conditioned on the image information only at the first time step. Vinyals *et al.* [58] combined deep CNNs for image classification with an LSTM for sequence modeling, to create a single network that generates descriptions of images. Xu *et al.* [62] proposed a model based on visual attention. Jia *et al.* [21] applied additional retrieved sentences to guide LSTM to generate captions.

Interestingly, this CNN-RNN end-to-end approach ignores the image-to-word mapping which was an essential step in many of the previous image captioning systems detailed above [15, 29, 37, 63]. The CNN-RNN approach has the advantage that it is able to generate a wider variety of captions, can be trained end-to-end, and outperforms the previous approach on the benchmarks. It is not clear, however, what the impact of bypassing the intermediate high-level representation is, and particularly to what extent the RNN language model might be compensating. Donahue *et al.* [12] describes an experiment, for example, using tags and CRF models as a mid-layer representation for video to generate descriptions, but it was designed to prove that LSTM outperforms an SMT-based approach [51]. It is still not clear whether the mid-layer representation or the LSTM leads to the success. Our paper provides several well-designed experiments to answer this question.

We thus here show not only a method for introducing a high-level representation into the CNN-RNN framework, and that doing so improves performance, but we also investigate the value of high-level information more broadly in *V2L* tasks. This is of critical importance at this time because *V2L* has a long way to go, particularly in the generality of the images and text it is applicable to.

Visual Question Answering Visual question answering is one of the more challenging, and interesting, *V2L* tasks as it requires answering previously unseen questions about image content [16, 39, 40, 41, 42, 50, 66]. This is as opposed to the vast majority of challenges in Computer Vision in which the question is specified long before the program is written. Both Gao *et al.* [16] and Malinowski *et al.* [42] used RNNs to encode the question and output the answer. Gao *et al.* [16] used two networks, a separate encoder and decoder while [42] used a single network. Ren *et al.* [50] focused on questions with a single-word answer and formulated the task as a classification problem using an LSTM and a single-word answer dataset COCO-QA was published with [50]. Ma *et al.* [39] used CNNs to both extract image features and sentence features, and fuse the features together with a multi-modal CNN. In contrast to the above approaches, we add an attributes layer to represent the image contents. Antol *et al.* [2] proposed a large-scale open-ended VQA dataset based on COCO, which is called COCO-VQA. We show that the proposed method achieves the state-of-the-art results on both COCO-QA and COCO-VQA datasets.

3 The Attribute-based *V2L* Model

Our approach is summarized in the Figure 1. The model includes an image understanding part and a language generation part. In the image understanding part, we first use supervised learning to predict a set of attributes, based on words commonly found in image captions. We treat this as a multi-label classification problem and train a corresponding deep CNN by minimizing an element-wise logistic loss function. Secondly, a fixed length vector $V_{att}(I)$ is created for each image I , whose length is the size of the attribute set. Each

dimension of the vector contains the prediction score for a particular attribute. In the language generation part, we apply an LSTM-based sentence generator. Our attributes vector $V_{att}(I)$ (red arrows in Figure 1) is used as an input to this LSTM. For different tasks, we have different designs of language models; for image captioning, we follow [58] to generate sentences from an LSTM; for single-word question answering, as in [50], we treat the LSTM as a classifier providing a likelihood for each potential answer; for open-ended question answering, we use an encoder LSTM to encode questions while the second LSTM decodes using the attribute vector $V_{att}(I)$ to generate a sentence based answer. A baseline model is also implemented for each of the three tasks. In the baseline model, as in [16, 50, 58] we use a pre-trained CNN to extract image features $CNN(I)$ and feed it into the LSTM directly. For the sake of completeness a fine-tuned version of this approach is also implemented. The baseline method is used as a counterpart to verify the effectiveness of the intermediate attribute prediction layer for each task.

3.1 Attribute Predictor

We label the set of attributes we seek within an image from a vocabulary. Unlike [29, 63], which use a vocabulary from separate hand-labeled training data, our semantic attributes are extracted from training captions and can be any part of speech, including object names (nouns), motions (verbs) or properties (adjectives). The direct use of captions guarantees that the most salient attributes for an image set are extracted. We use the c most common words in the training captions to determine the attribute vocabulary \mathcal{V}_{att} . Different with [13], our vocabulary is not tense or plurality sensitive, for instance, ‘ride’ and ‘riding’ are classified as the same semantic attribute, similarly ‘bag’ and ‘bags’. This significantly decreases the size of our attribute vocabulary. Moreover, in contrast to Fang *et al.* [13], who directly use the words in the attribute vocabulary to construct a sentence, our attributes represent a set of high-level semantic constructs, the totality of which the LSTM then attempts to represent in sentence form. Generating a sentence from a vector of attribute likelihoods exploits a much larger set of candidate words which are learned separately, allowing for significantly greater flexibility in the generated text (see Section 3.2).

Given this attribute vocabulary, we can associate each image with a set of attributes according to its captions. We then wish to predict the attributes given a test image. Because we do not have ground truth bounding boxes for attributes, we cannot train a detector for each using the standard approach. Fang *et al.* [13] solved a similar problem using a Multiple Instance Learning framework [65] to detect visual words from images. Motivated by the relatively small number of times that each word appears in a caption, we instead treat this as a multi-label classification problem. To address the concern that some attributes may only apply to image sub-regions, we follow Wei *et al.* [60] in designing a region-based multi-label classification framework that take an arbitrary number of sub-regions proposals as input, then a shared CNN is connected with each proposal, and the CNN output results from different proposals are aggregated with max pooling to produce the final prediction.

Figure 2 summarized the attribute prediction network. In contrast to [60], who used AlexNet [28] as the initialization of the shared CNN, we use the more powerful VGGNet [52] pre-trained on ImageNet[11]. This model has been widely used in image captioning tasks[13, 43, 25]. The shared CNN is then fine-tuned on the target multi-label dataset, our image-attribute training data. In this step, the output of the last fully-connected layer is fed into a c -way softmax which produces a probability distribution over the c class labels. The c here represents the vocabulary size. In contrast to [60] who employed the squared loss, we instead use an element-wise logistic loss function. Suppose there are N training examples and $\mathbf{y}_i = [y_{i1}, y_{i2}, \dots, y_{ic}]$ is the label vector of the i^{th} image where $y_{ij} = 1$ if the image is annotated with attribute j , and $y_{ij} = 0$ otherwise. If the predictive probability vector is $\mathbf{p}_i = [p_{i1}, p_{i2}, \dots, p_{ic}]$, then the cost function to be minimized is

$$J = \frac{1}{N} \sum_{i=1}^N \sum_{j=1}^c \log(1 + \exp(-y_{ij}p_{ij})) \quad (1)$$

During the fine-tuning process the parameters of the last fully connected layer (i.e. the attribute prediction layer) are initialized with a Xavier initialization [17]. The learning rates of **fc6** and **fc7** are initialized as 0.001 and the last fully connected layer is initialized as 0.01. All the other layers are fixed during training. We executed 40 epochs in total and decreased the learning rate to one tenth of the current rate for each layer after 10 epochs. The momentum is set to 0.9. The dropout rate is set to 0.5.

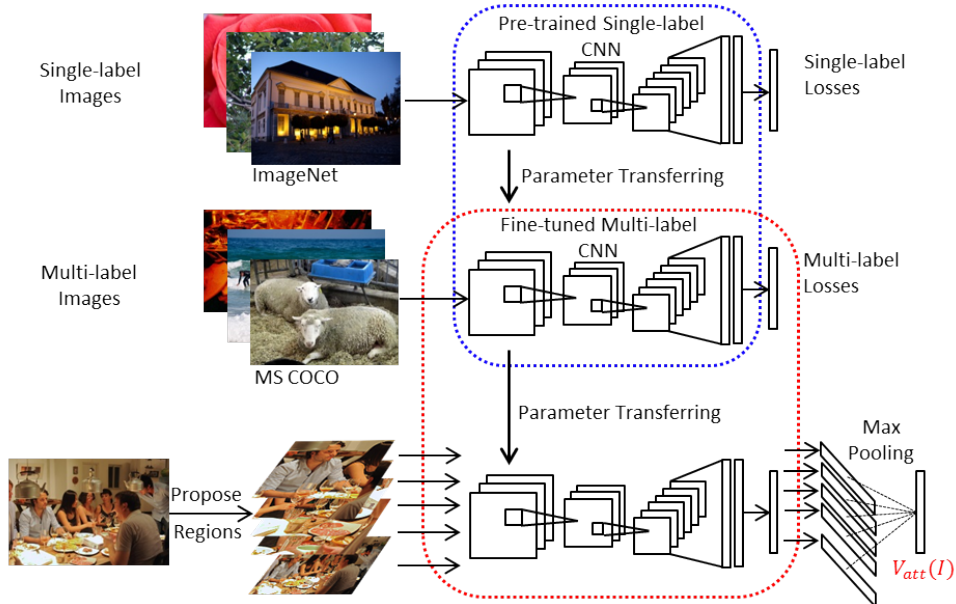


Figure 2 – Attribute prediction CNN: the model is initialized from a VGGNet [52] pre-trained on ImageNet. Secondly, it is fine-tuned on the target multi-label dataset. Given a test image, a set of proposal regions are selected and passed to the shared CNN, and finally the CNN outputs from different proposals are aggregated with max pooling to produce the final multi-label prediction, which gives us the high-level image representation, $V_{att}(I)$

To predict attributes based on regions, we first extract hundreds of proposal windows from an image. However, considering the computational inefficiency of deep CNNs, the number of proposals processed needs to be minimized. Similar to [60], we first apply the normalized cut algorithm to group the proposal bounding boxes into m clusters based on the IoU scores matrix. The top k hypotheses in terms of the predictive scores reported by the proposal generation algorithm are kept and fed into the shared CNN. In contrast to [60], we also include the whole image in the hypothesis group. As a result, there are $mk + 1$ hypotheses for each image. We set $m = 10, k = 5$ in all experiments. We use Multiscale Combinatorial Grouping (MCG) [49] for the proposal generation. Finally, a cross hypothesis max-pooling is applied to integrate the outputs into a single prediction vector $V_{att}(I)$.

3.2 Language Generator

Similar to [25, 43, 58], we propose to train a language generation model by maximizing the probability of the correct description given the image. However, rather than using image features directly as in typically the case, we use the semantic attribute prediction scores $V_{att}(I)$ from the previous section as the input. Suppose $\{S_1, \dots, S_L\}$ is a sequence of words. The log-likelihood of the words given their context words and the corresponding image can be written as:

$$\log p(S|V_{att}(I)) = \sum_{t=1}^L \log p(S_t|S_{1:t-1}, V_{att}(I)) \quad (2)$$

where $p(S_t|S_{1:t-1}, V_{att}(I))$ is the probability of generating the word S_t given attribute vector $V_{att}(I)$ and previous words $S_{1:t-1}$. We employ the LSTM [19], a particular form of RNN, to model this. LSTM is a memory cell, for every time step, encodes a representation of the inputs have been observed up to this step. See Figure 3 for different language generators designed for multiple $V2L$ tasks.

Image Captioning Model The LSTM model for image captioning is trained in an unrolled form. More formally, the LSTM takes the attributes vector $V_{att}(I)$ and a sequence of words $S = (S_0, \dots, S_L, S_{L+1})$, where S_0 is a special start word ‘.’ and S_{L+1} is a special END token. Each word has been represented as a one-hot

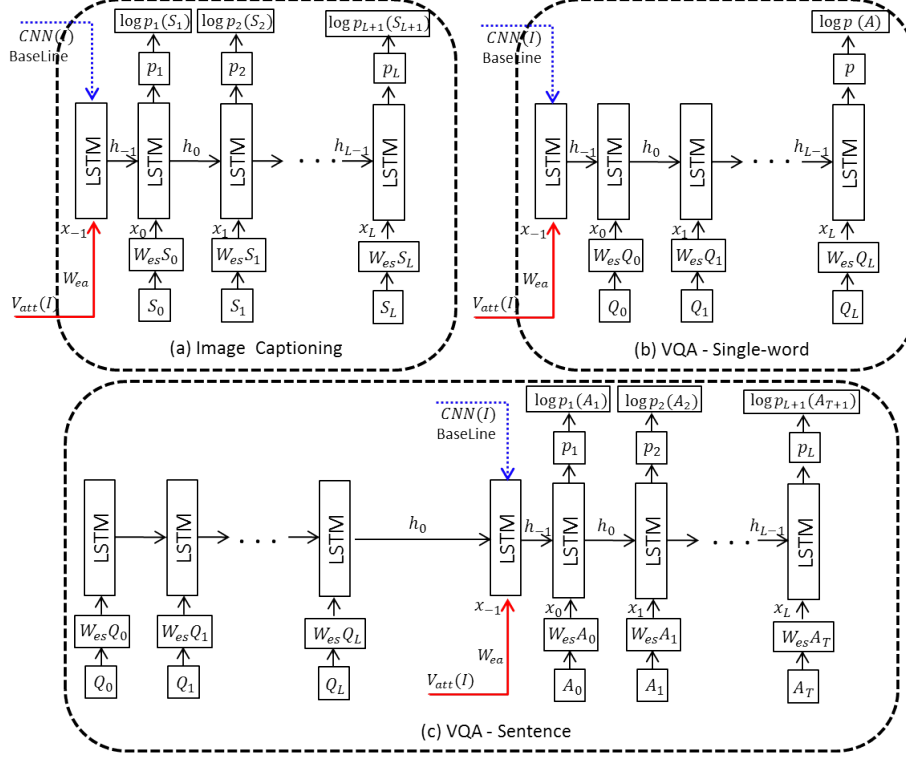


Figure 3 – Language generators for different types of tasks: (a) Image Captioning, (b) VQA-single word, (c) VQA-sentence. red arrow indicates our attributes input $V_{att}(I)$ while blue dash arrow shows the baseline method input $CNN(I)$.

vector S_t of dimension equal to the size of words dictionary. The words dictionaries are build based on words that occur at least 5 times in the training set, which lead to 2538, 7414, and 8791 words on Flickr8k, Flickr30k and MS COCO datasets separately. Noting it is different from the semantic attributes vocabulary \mathcal{V}_{att} . The training procedure is as following (see Figure 3 (a)) : At time step $t = -1$, we set $x_{-1} = W_{ea}V_{att}(I)$ and $h_{initial} = \vec{0}$, where W_{ea} is the learnable attributes embedding weights. This gives us an initial LSTM hidden state h_{-1} which can be used in the next time step. From $t = 0$ to $t = L$, we set $x_t = W_{es}S_t$ and the hidden state h_{t-1} is given by the previous step, where W_{es} is the learnable word embedding weights. The probability distribution p_{t+1} over all words is then computed by the LSTM feed-forward process. Finally, on the last step when S_{L+1} represents the last word, the target label is set to the END token.

Our training objective is to learn parameters W_{ea} , W_{es} and all parameters in LSTM by minimizing the following cost function:

$$\begin{aligned}
\mathcal{C} &= -\frac{1}{N} \sum_{i=1}^N \log p(S^{(i)} | V_{att}(I^{(i)})) + \lambda_{\theta} \cdot \|\theta\|_2^2 \\
&= -\frac{1}{N} \sum_{i=1}^N \sum_{t=1}^{L^{(i)}+1} \log p_t(S_t^{(i)}) + \lambda_{\theta} \cdot \|\theta\|_2^2
\end{aligned} \tag{3}$$

where N is the number of training examples and $L^{(i)}$ is the length of the sentence for the i -th training example. $p_t(S_t^{(i)})$ corresponds to the activation of the Softmax layer in the LSTM model for the i -th input and θ represents model parameters, $\lambda_{\theta} \cdot \|\theta\|_2^2$ is a regularization term. We use SGD with mini-batches of 100 image-sentence pairs. The attributes embedding size, word embedding size and hidden state size are all set to 256 in all the experiments. The learning rate is set to 0.001 and clip gradients is 5. The dropout rate is set to 0.5.

Question Answering Model For question answering, a triplet $\{V_{att}(I), \{Q_1, \dots, Q_L\}, \{A_1, \dots, A_T\}\}$ will be given, whereas L and T is the length of the question and answer, separately. We define it is a single-word answering problem when $T = 1$ and it is a sentence-based problem if $T > 1$.

For the single-word answering problem, the LSTM takes the attributes score vector $V_{att}(I)$ and a sequence of input words of the question $Q = (Q_1, \dots, Q_L)$. The feed-forward process is same as image captioning, except that an END token is not required anymore. Instead, we treat the word generated by the last word of the question as the predicted answer (see Figure 3 (b)). Hence, the cost function is $\mathcal{C} = -\frac{1}{N} \sum_{i=1}^N \log p(A^{(i)}) + \lambda_{\theta} \cdot \|\theta\|_2^2$, where N is the number of training examples and i is the i -th training example. $\log p(A^{(i)})$ is the log-probability distribution over all candidate answers that is computed by the last LSTM cell, given the previous hidden state and the last word of question Q_L .

For the sentence-based question answering, we have a question encoding LSTM and an answer decoding LSTM. However, different from Gao *et al.* [16] using two separates LSTMs for question and answer, weights between our encoding and decoding LSTMs are shared. The information stored in the LSTM memory cells of the last word in the question is treated as the representation of the sentence. And its hidden state will be used as the initial state of the answering LSTM part. Moreover, different from [16, 42, 50] who use CNN features directly, we use our attributes representations $V_{att}(I)$ as the input for decoding LSTM (see Figure 3 (c)). The cost function of sentence-based question answering is $\mathcal{C} = -\frac{1}{N} \sum_{i=1}^N \sum_{t=1}^{T^{(i)}+1} \log p_t(A_t^{(i)}) + \lambda_{\theta} \cdot \|\theta\|_2^2$, where $T^{(i)} + 1$ is the length of the answer plus one END token for the i -th training example. According to training configuration, the learning rate is set to 0.0005 and other parameters are same as image captioning configuration.

4 Image Captioning

4.1 Dataset

There are several datasets which consist of images and sentences in English describing these images. We report results on the popular Flickr8k [20], Flickr30k [64] and Microsoft COCO dataset [38]. These datasets contain 8,000, 31,000 and 123,287 images respectively, and each image is annotated with 5 sentences. In our reported results, we use pre-defined splits for Flickr8k, 1000 for validation, 1000 for testing and the rest for training. Because most of previous works in image captioning [12, 13, 25, 43, 58, 62] are not evaluated on the official split for Flickr30k and MS COCO, for fair comparison, we report results with the widely used publicly available splits in the work of [25], which use 1000 images for validation, 1000 for testing for Flickr30k, and 5000 images for both validation and testing in MS COCO. We further tested on the actually MS COCO test set (official split) consisting of 40775 images (human captions for this split are not available publicly), and evaluated them on the COCO evaluation server.

4.2 Evaluation

Metrics We report results with the frequently used BLEU metric and sentence perplexity (\mathcal{PPL}). BLEU [48] scores are originally designed for automatic machine translation where they measure the fraction of N-grams (up to 4-gram) that are in common between a hypothesis and a reference or set of references. Here we compare against 5 references. The perplexity (\mathcal{PPL}) is a standard measure for evaluating language models. It measures how many bits on average would be needed to encode each word given the language model, so a low \mathcal{PPL} means a better language model. For MS COCO dataset, we additionally evaluate our model based on the metrics of METEOR [5] and CIDEr [57]. All scores (except \mathcal{PPL}) are computed with the `coco-caption` code [7].

Baselines To verify the effectiveness of our high-level attributes representation, we provide a baseline method. The baseline framework is same as the one proposed in section 3.2, except that the attributes vector $V_{att}(I)$ is replaced by the last hidden layer of CNN $CNN(I)$ directly (see the blue arrow in Figure 3). Various CNN architectures are applied in the baseline method to extract image features, such as VggNet[52] and GoogLeNet[56]. For the **VggNet+LSTM**, we use the second fully connected layer (`fc7`) as the image features, which has 4096 dimensions. In **VggNet-PCA+LSTM**, a PCA is applied to decrease the feature

Flickr8k					
State-of-art-Flickr8k	B-1	B-2	B-3	B-4	\mathcal{PPL}
Karpathy & Li (NeuralTalk) [25]	0.58	0.38	0.25	0.16	-
Chen & Zintick (Mind’s Eye) [8]	-	-	-	0.14	15.10
Google(NIC)[58]	0.66	0.42	0.27	0.18	-
Mao et al. (m-Rnn-AlexNet) [43]	0.57	0.39	0.26	0.17	24.39
Xu et al. (Hard-Attention) [62]	0.67	0.46	0.31	0.21	-
Baseline - CNN(I)					
VggNet+LSTM	0.56	0.37	0.24	0.16	15.71
VggNet-PCA+LSTM	0.56	0.38	0.25	0.16	16.07
GoogLeNet+LSTM	0.56	0.38	0.24	0.16	15.71
VggNet+ft+LSTM	0.64	0.43	0.30	0.20	14.69
Ours - $V_{att}(I)$					
Attributes-GT+LSTM [‡]	0.76	0.57	0.41	0.29	12.52
Attributes-SVM+LSTM	0.73	0.53	0.38	0.26	12.63
Attributes-CNN+LSTM	0.74	0.54	0.38	0.27	12.60

Flickr30k					
State-of-art-Flickr30k	B-1	B-2	B-3	B-4	\mathcal{PPL}
Karpathy & Li (NeuralTalk) [25]	0.57	0.37	0.24	0.16	-
Chen & Zintick (Mind’s Eye) [8]	-	-	-	0.13	19.10
Google(NIC) [58]	0.66	-	-	-	-
Donahue et al. (LRCN) [12]	0.59	0.39	0.25	0.17	-
Mao et al. (m-Rnn-AlexNet) [43]	0.54	0.36	0.23	0.15	35.11
Mao et al. (m-Rnn-VggNet) [43]	0.60	0.41	0.28	0.19	20.72
Xu et al. (Hard-Attention) [62]	0.67	0.44	0.30	0.20	-
Baseline - CNN(I)					
VggNet+LSTM	0.57	0.38	0.25	0.17	18.83
VggNet-PCA+LSTM	0.59	0.40	0.26	0.17	18.92
GoogLeNet+LSTM	0.58	0.39	0.26	0.17	18.77
VggNet+ft+LSTM	0.67	0.47	0.31	0.21	16.62
Ours - $V_{att}(I)$					
Attributes-GT+LSTM [‡]	0.78	0.57	0.42	0.30	14.88
Attributes-SVM+LSTM	0.68	0.49	0.33	0.23	16.01
Attributes-CNN+LSTM	0.73	0.55	0.40	0.28	15.96

Table 1 – BLEU-1,2,3,4 and \mathcal{PPL} metrics compared to other state-of-the-art methods and our baseline on Flickr8k and Flickr30K dataset. ‡ indicates ground truth attributes labels are used, which (in gray) will not participate in rankings. Our \mathcal{PPL} s are based on Flickr8k and Flickr30k word dictionaries of size 2538 and 7414, respectively.

dimension from 4096 to 1000. For the **GoogLeNet+LSTM**, we use the model provided in the Caffe Model Zoo [23] and the last average pooling layer is employed, which is a 1024-d vector. **VggNet+ft+LSTM** applies a VggNet that has been fine-tuned on the target dataset, based on the task of image-attributes classification.

Our Approaches We evaluate several variants of our approach: **Attributes-GT+LSTM** models use ground-truth attributes labels as the input while **Attributes-CNN+LSTM** uses the attributes vector $V_{att}(I)$ predicted by the attributes prediction network in section 3.1. We also evaluate an approach **Attributes-SVM+LSTM** with whole image attributes prediction using standard SVM. Image features that are used to build SVM classifiers are from VGGNet and have been fine-tuned on the target dataset. To infer the sentence given an input image, we iteratively consider the set of b best sentences up to time t as candidates to generate sentences at time $t + 1$, and only keep the best b results. We set the beam size b as 5 in all experiments.

State-of-art	B-1	B-2	B-3	B-4	M	C	\mathcal{P}
NeuralTalk [25]	0.63	0.45	0.32	0.23	0.20	0.66	-
Mind’s Eye [8]	-	-	-	0.19	0.20	-	11.60
NIC [58]	-	-	-	0.28	0.24	0.86	-
LRCN [12]	0.67	0.49	0.35	0.25	-	-	-
Mao et al.[43]	0.67	0.49	0.34	0.24	-	-	13.60
Jia et al.[21]	0.67	0.49	0.36	0.26	0.23	0.81	-
MSR [13]	-	-	-	0.26	0.24	-	18.10
Xu et al.[62]	0.72	0.50	0.36	0.25	0.23	-	-
Jin et al.[24]	0.70	0.52	0.38	0.28	0.24	0.84	-
Baseline-$CNN(I)$							
VNet+LSTM	0.61	0.42	0.28	0.19	0.19	0.56	13.58
VNet-PCA+LSTM	0.62	0.43	0.29	0.19	0.20	0.60	13.02
GNet+LSTM	0.60	0.40	0.26	0.17	0.19	0.55	14.01
VNet+ft+LSTM	0.68	0.50	0.37	0.25	0.22	0.73	13.29
Ours-$V_{att}(I)$							
Att-GT+LSTM [‡]	0.80	0.64	0.50	0.40	0.28	1.07	9.60
Att-SVM+LSTM	0.69	0.52	0.38	0.28	0.23	0.82	12.62
Att-CNN+LSTM	0.74	0.56	0.42	0.31	0.26	0.94	10.49

Table 2 – BLEU-1,2,3,4, METEOR, CIDEr and \mathcal{PPL} metrics compared to other state-of-the-art methods and our baseline on MS COCO dataset. ‡ indicates ground truth attributes labels are used, which (in gray) will not participate in rankings. Our \mathcal{PPL} s are based on MS COCO word dictionaries of size 8791.

Results Table 1 and 2 report image captioning results on Flickr8k, Flickr30k and Microsoft COCO dataset. The **Attributes-GT+LSTM** models perform best over all datasets and all evaluation metrics. Although the outstanding performance relies on using ground truth attributes labels, we report these results here just to show the advances of adding an intermediate image-to-word mapping stage. Ideally, if we are able to train a strong attributes predictor which gives us a good enough estimation of attributes, we could obtain an outstanding improvement comparing with both baselines and state-of-the-arts. Indeed, apart from using ground truth attributes, our **Attributes-CNN+LSTM** models generate the best results on all the three datasets over all evaluation metrics. Especially comparing with baselines, which do not contain an attributes prediction layer, our final models bring significant improvements, nearly 15% for B-1 and 30% for CIDEr on average. **VggNet+ft+LSTM** models perform better than other baselines because of the fine-tuning on the target dataset. However, they do not perform as good as our attributes-based models. **Attributes-SVM+LSTM** under-perform **Attributes-CNN+LSTM** means our region-based attributes prediction network performs better than the whole image classification. Our final model also outperforms current state-of-the-arts listed in tables. We also evaluate an approach (not shown in table) that combines CNN features and attributes vector together as the input of the LSTM, but we find this approach is not as good as using attributes vector only in the same setting. In any case, above experiments show that an intermediate image-to-words stage (i.e. attributes prediction layer) bring us significant improvements.

We further generated captions for the images in the COCO test set containing 40,775 images and evaluated them on the COCO evaluation server. These results are shown in table 3. We achieve 0.73 on B-1, and surpasses human performances on 13 of the 14 metrics reported. We are the best results on 3 evaluations metrics (B-1,2,3) on the server leaderboard at the time of written this paper. We also achieve the top-5 ranking on the other evaluation metrics.

Table 4 summarize some properties of the recurrent layers employed in the some recent RNN-based methods. We achieve state-of-the-art using a relatively small dimensional visual input feature and recurrent layer. Lower dimension of visual input and RNN normally means less parameters in the RNN training stage, as well as lower computation cost.

COCO-TEST	B-1	B-2	B-3	B-4	M	R	CIDEr
5-Refs							
Ours	0.73	0.56	0.41	0.31	0.25	0.53	0.92
Human	0.66	0.47	0.32	0.22	0.25	0.48	0.85
MSR [13]	0.70	0.53	0.39	0.29	0.25	0.52	0.91
m-RNN [43]	0.68	0.51	0.37	0.27	0.23	0.50	0.79
LRCN [12]	0.70	0.53	0.38	0.28	0.24	0.52	0.87
40-Refs							
Ours	0.89	0.80	0.69	0.58	0.33	0.67	0.93
Human	0.88	0.74	0.63	0.47	0.34	0.63	0.91
MSR [13]	0.88	0.79	0.68	0.57	0.33	0.66	0.93
m-RNN [43]	0.87	0.76	0.64	0.53	0.30	0.64	0.79
LRCN [12]	0.87	0.77	0.65	0.53	0.32	0.66	0.89

Table 3 – COCO evaluation server results on test set (40775 images). M and R stands for METEOR and ROUGE-L. Results using 5 reference and 40 references captions are both shown, with human performances. We only report previous work when the results have been officially published in the corresponding references.

	Ours	NIC[58]	LRCN[12]	m-RNN[43]	NeuralTalk[25]
VIS Input Dim	256	1000	1000	4096	4096
RNN Dim	256	512	1000×4	256	300-600

Table 4 – Visual feature input dimension and properties of RNN. Our visual features has been encoded as a 256-d attributes score vector while other models need higher dimensional features to feed to RNN. According to the unit size of RNN, we achieve state-of-the-art using a relatively small dimensional recurrent layer.

5 Visual Question Answering

5.1 Dataset

We report VQA results on two recently publicly available visual question answering dataset, both are created based on MS COCO. Toronto COCO-QA Dataset [50] contains 78,736 training and 38,948 testing examples, which are generated from 117,684 images. There are four types of questions, specifically the object, number, color and location. The answers are all single-word. We use this dataset to examine our single-word question answering model. MS COCO-VQA [2] is a much larger dataset which contains 369,861 questions and 3,698,610 answers based on 123,287 COCO images. These questions and answers are sentence-based and open-ended. The training and testing split follows COCO official split, which contains 82,783 training images and 40,504 validation images, each has 3 questions and 10 answers. We randomly choose 5000 images from validation as our val set, while others are used as testing.

5.2 Evaluation

Same as image captioning, our experiments in question answering is designed for verifying the effectiveness of introducing the intermediate attributes layer. Hence, except listing several state of arts, we focus on comparing with a baseline method, which only uses the last hidden layer of a pre-trained VggNet as the input.

Table 5 reports results on the COCO-QA dataset, whose answers are single-word. Besides the accuracy value (the proportion of correct answered testing questions to the total testing questions), the Wu-Palmer similarities (WUPS) [61] is also used to measure the performance of different models. The WUPS calculates the similarity between two words based on the similarity between two words based their common subsequence in the taxonomy tree. If the similarity between two words is bigger than a threshold then the candidate answer is supposed to be right. We follow [39, 50] setting the threshold as 0.9 and 0.0. **GUESS** is a simple baseline to predict the mode based on the question type. The modes are ‘cat’, ‘two’, ‘white’, and ‘room’ corresponding to four types of questions. **VIS+BOW** [50] performs multinomial logistic regression based on image features and an BOW vector obtained by summing all the word vectors of the question. **VIS+LSTM**

COCO-QA	Acc	WUPS@0.9	WUPS@0.0
GUESS[50]	6.65	17.42	73.44
VIS+BOW[50]	55.92	66.78	88.99
VIS+LSTM[50]	53.31	63.91	88.25
2-VIS+BLSTM[50]	55.09	65.34	88.64
Ma et al.[39]	54.94	65.36	88.58
BaseLine			
VggNet-LSTM	50.73	60.37	87.48
Our-Proposal			
Attributes-GT+LSTM [‡]	67.66	75.76	93.63
Attributes-CNN+LSTM	61.38	71.15	91.58

Table 5 – Accuracy, WUPS@0.9 and WUPS@0.0 metrics compared to other state-of-the-art methods and our baseline on COCO-QA dataset. Each image has one question and only a single word answer is given for each question. ‡ indicates ground truth attributes labels are used, which will not participate in rankings.

[50] has one LSTM to encode the image and question, while **2-VIS+BLSTM** has two image features input, at the start and the end of the sentences. Ma *et al.* encoded images and questions both with CNN. From the table 5, we clearly see that our attributes-based model outperforms baselines and all the state-of-the-arts in a significant degree, which proves the effectiveness of our attribute-based representation.

Table 6 summarizes the results on MS COCO-VQA dataset, which we used to measure our sentence question answering model. Different with evaluation metrics used in above single-word question answering task, here we follow [2], recording the percentage of answers on agreement with ground truth from human subjects. Antol *et al.* [2] provided a baseline for this dataset using a **CNN+BOW** method, which encodes the image with CNN features and questions with BOW representation. Then they train a softmax neural network classifier with a single hidden layer containing 50 units and the output space are 500 most frequent answers in the training set. A human performance is also given in [2] for reference. From the results, we can see our attributes model surpass VQA-Baseline on all question types and the overall accuracy increase nearly 25%. We outperforms our baseline **VGG+LSTM** except the question type start with ‘do’. It is surprising that our attributes-based model even outperforms Human on the ‘what sport’ type questions (91.02 VS 80.18). Actually, we have a dramatically increase on questions start with ‘what’ (such as ‘what is’, ‘what color’, ‘what sport’, ‘what animal’ .etc.) when switching on our attributes prediction layers. It is mainly because the information (such as object names, colors, types), which is necessary for answering these types of questions, has been encoded in our attributes prediction layer. In other words, the high-level semantic representation provides more explicit information than hidden layers in the CNN. Once again, we prove the effectiveness of introducing an image-to-words mappings (which has been ignored in current CNN+RNN frameworks) in *V2L* tasks.

However, we also noticed that accuracies on some question types such as ‘why’ are very low. This kinds of questions are hard to answer because commonsense knowledge and reasoning is normally required, which suggests that higher level information such as knowledge base need to be encoded with questions and images. Zhu *et al.* [66] cast a MRF model into a KB representation to answer commonsense-related visual questions. Our semantic attributes representation enables us to fetch higher-level knowledge-based informations beyond images since all existing knowledge bases (such as DBpedia[3], Freebase[6]) are using semantic words, but not images, as KB entities. In the following experiment, we propose to expand our image-based attributes set to a knowledge-based attributes set through a large lexical ontology - the WordNet[45].

5.3 Attributes Expansion using WordNet

The WordNet [45] provides abundant relationships between words. The most frequently encoded relation is the hyponymy (such as **bed** and **bunkbed**). Meronymy represents the part-whole relation (**seat** and **leg**). Verb synsets are arranged into hierarchies (troponyms) as well (such as **communicate-talk-whisper**, **buy-pay**, **succeed-try**). Adjectives are organized in terms of both synonymy and antonymy. All these relationships are defined based on commonsense and human knowledges. To quantify them, we further apply the word2vec [44] to measure the semantic similarity between two words.

Question Type	VQA-BL	Our-BL	Our Proposal		Human [2]
	CNN	VGG	Att-CNN	Att-GT	
	+	+	+	+	
	BOW [2]	LSTM	LSTM	LSTM‡	
what is	7.05	21.41	34.63	38.45	47.11
what colour	17.05	29.96	39.07	46.16	65.65
what kind	5.02	24.15	41.22	45.35	39.98
what are	8.59	23.05	38.87	41.96	45.36
what type	8.50	26.36	41.71	46.11	40.62
is the	52.27	71.49	73.22	73.93	83.37
is this	51.49	73.00	75.26	76.37	81.82
how many	27.25	34.42	39.14	44.20	64.43
are	55.01	73.51	75.14	75.75	83.39
does	58.79	76.51	76.71	77.17	82.78
where	2.23	10.54	21.42	21.45	20.82
is there	72.55	86.66	87.10	86.86	84.36
why	3.42	3.04	7.77	8.49	8.21
which	17.86	31.28	36.60	37.83	39.76
do	58.33	76.04	75.76	75.91	80.48
what does	7.19	15.45	19.33	19.74	50.26
what time	5.56	13.11	15.34	15.84	30.84
who	8.02	17.07	22.56	23.47	30.89
what sport	55.99	65.65	91.02	92.75	80.18
what animal	17.61	27.77	61.39	64.26	75.83
what brand	5.76	26.73	32.25	32.63	59.68
others	-	44.37	50.23	52.00	-
Overall	27.13	44.93	51.60	54.10	61.58

Table 6 – Results on the open-answer task for various question types on MS COCO-VQA. There are three questions for each image. All results are the percentage of answers in agreement with human subjects and evaluation metric is from COCO-VQA evaluation tools [2]. ‡ indicates ground truth attributes labels are used. Human results [2] are also reported for reference.

To expand our image-sourced attributes to knowledge-sourced, we first select candidate words from the WordNet. Candidate words must fulfill two selection criteria. The first is the candidate word must have one of the above WordNet relationships with an arbitrary word in our attributes vocabulary \mathcal{V}_{att} . Secondly, the candidate word must be appeared in at least 5 training question examples. In our experiment, given $M = 256$ image-sourced attributes and the COCO-VQA dataset, we finally mined a knowledge-sourced vocabulary \mathcal{V}_{kb} with $N = 9762$ words, and \mathcal{V}_{kb} covers all the words in \mathcal{V}_{att} . Then, a similarity matrix $S \in \mathbb{R}^{M \times N}$ is computed based on a pre-trained word2vec model [44], where S_{ij} gives the both semantic and syntactic similarity between word i in \mathcal{V}_{att} and word j in \mathcal{V}_{kb} .

Given an image I and its image-sourced attributes vector $V_{att}(I) = (v_{att}^{(1)}, \dots, v_{att}^{(i)}, \dots, v_{att}^{(M)})$ predicted by the attributes prediction network, the j^{th} component of the knowledge-sourced attributes vector is obtained by a max-pooling operator $v_{kb}^{(j)} = \max(v_1^{(j)}, \dots, v_i^{(j)}, \dots, v_M^{(j)})$, where $v_i^{(j)} = v_{att}^{(i)} \times S_{ij}$. The final knowledge-sourced attributes vector $V_{kb}(I) = (v_{kb}^{(1)}, \dots, v_{kb}^{(j)}, \dots, v_{kb}^{(N)})$, will be fed into the LSTM to generate answers.

Table 7 compares results of using image-sourced attributes VS knowledge-sourced on the COCO-VQA dataset. We gain a significant improvement on commonsense reasoning related questions. For example, on the ‘why’ types questions, we achieve 9.26%, even better than human performance 8.21%. This is not surprising since some commonsense knowledge has been encoded into our expanded knowledge-sourced attributes vectors. Our work point a new direction of combining KB and question answering tasks. According to the overall result, we achieve 53.59% accuracy, which is the best reported result on the COCO-VQA.



- Top -5 Attributes
- couch, sleeping , brown, laying, dog
- Question Answering
- Does this animal appear to be resting ?
 - yes (**yes**)
 - What is the color of the cushions ?
 - brown (**brown**)

Generated caption

- a dog laying on top of a couch next to a pillow.



- Top -5 Attributes
- group, people, children, cake, grass
- Question Answering
- What kind of event does this look like?
 - birthday party (**birthday**)
 - Is this woman trying to give the kids an uncooked cake?
 - no (**no**)

Generated caption

- a group of children standing around a cake.



- Top -5 Attributes
- top, cake, fruits, table, plates
- Question Answering
- What are the orange sticks?
 - carrots (**carrots**)
 - How many carrots are in the bowls?
 - 2 (**over 10**)
 - Is this set up for a party?
 - yes (**yes**)

Generated caption

- a table topped with plates of food.



- Top -5 Attributes
- jumping, watching, skate, board, people
- Question Answering
- What is the guy doing?
 - skateboarding (**skateboarding**)
 - Are both of these skateboarders upside down?
 - yes (**no**)
 - Why are there signs on the wall?
 - to keep clean (**advertising**)

Generated caption

- a man doing a trick on a skateboard.



- Top -5 Attributes
- shelf, small, book, room, television
- Question Answering
- What pattern is on the curtain?
 - floral (**leaves**)
 - What sport is being displayed on the television?
 - football (**football**)
 - Is there a bookcase nearby?
 - yes (**yes**)

Generated caption

- a living room with a couch and a television.

Figure 4 – Qualitative results for images in the Microsoft COCO dataset. Top-5 predicted attributes, question answering examples and our generated captions are given for each image. Ground truth answers are in parentheses. Blue indicates we gave the right answer while red means we are wrong.

Question-Type	$V_{att}(I)+LSTM$	$V_{kb}(I)+LSTM$	Human[2]
why	7.77	9.26	8.21
what kind	41.22	45.23	39.98
which	36.60	37.28	39.76
is the	73.22	74.56	83.37
is this	75.26	76.61	81.82
overall (all types)	51.60	53.59	61.58

Table 7 – Results on the open-answer task for some commonsense reasoning question types on MS COCO-VQA. ‘overall’ is calculated based on all types of questions. Human results [2] are also reported for reference.

6 Conclusion

This paper discusses a fundamental question: *is it really beneficial to bypass the image-to-words mappings in V2L tasks?* This question is raised since many recent papers in this area are bias to ignore image-to-words mappings, while a large number of conventional works treat it as a necessary step. To answer this question, we examine the effect of introducing an intermediate attributes prediction layer into the famous CNN-LSTM framework. We implement three attributes-based models for the task of image captioning, single-word question answering and sentence question answering, respectively.

Although learning an image-to-sentence end to end model is an attractive and popular approach, all of our experiments clearly prove that ignoring the image-to-words mapping leads to a decrease in a serious of V2L tasks when comparing with using an attributes prediction layer as the high-level representation. Indeed, at the time of the submission, our image captioning model produces the best results on the COCO image captioning task, comparing with state-of-the-arts. Our question answering models performs best on two VQA datasets. We also provide the first state-of-the-art on the MS COCO-VQA, achieving 53.59% accuracy, while the baseline is 27.13% and human performance reaches 61.58%. Moreover, attributes representation enables us to access high-level commonsense knowledges, which is necessary for answering commonsense reasoning related questions. Our work not only prove the value of the attributes layer, but also leads to a new way of combing KB in the V2L tasks.

References

- [1] A. Aker and R. Gaizauskas. Generating image descriptions using dependency relational patterns. In *ACM Trans. of the Association for Computational Linguistics*, 2010.
- [2] S. Antol, A. Agrawal, J. Lu, M. Mitchell, D. Batra, C. L. Zitnick, and D. Parikh. VQA: Visual Question Answering. *arXiv preprint arXiv:1505.00468*, 2015.
- [3] S. Auer, C. Bizer, G. Kobilarov, J. Lehmann, R. Cyganiak, and Z. Ives. *Dbpedia: A nucleus for a web of open data*. Springer, 2007.
- [4] D. Bahdanau, K. Cho, and Y. Bengio. Neural machine translation by jointly learning to align and translate. *arXiv:1409.0473*, 2014.
- [5] S. Banerjee and A. Lavie. METEOR: An automatic metric for MT evaluation with improved correlation with human judgments. In *Proc. ACL workshop on intrinsic and extrinsic evaluation measures for machine translation and/or summarization*, 2005.
- [6] K. Bollacker, C. Evans, P. Paritosh, T. Sturge, and J. Taylor. Freebase: a collaboratively created graph database for structuring human knowledge. In *Proc. ACM SIGMOD international conference on Management of data*, pages 1247–1250. ACM, 2008.
- [7] X. Chen, H. Fang, T.-Y. Lin, R. Vedantam, S. Gupta, P. Dollar, and C. L. Zitnick. Microsoft COCO captions: Data collection and evaluation server. *arXiv:1504.00325*, 2015.
- [8] X. Chen and C. Lawrence Zitnick. Mind’s Eye: A Recurrent Visual Representation for Image Caption Generation. In *Proc. IEEE Conf. Comp. Vis. Patt. Recogn.*, June 2015.
- [9] X. Chen and C. L. Zitnick. Learning a Recurrent Visual Representation for Image Caption Generation. In *Proc. IEEE Conf. Comp. Vis. Patt. Recogn.*, 2015.
- [10] K. Cho, B. van Merriënboer, C. Gulcehre, F. Bougares, H. Schwenk, and Y. Bengio. Learning phrase representations using rnn encoder-decoder for statistical machine translation. In *Proc. Conf. Empirical Methods on Natural Language Processing*, 2014.
- [11] J. Deng, W. Dong, R. Socher, L.-J. Li, K. Li, and L. Fei-Fei. Imagenet: A large-scale hierarchical image database. In *Proc. IEEE Conf. Comp. Vis. Patt. Recogn.*, 2009.
- [12] J. Donahue, L. A. Hendricks, S. Guadarrama, M. Rohrbach, S. Venugopalan, K. Saenko, and T. Darrell. Long-term recurrent convolutional networks for visual recognition and description. In *Proc. IEEE Conf. Comp. Vis. Patt. Recogn.*, 2015.
- [13] H. Fang, S. Gupta, F. Iandola, R. Srivastava, L. Deng, P. Dollár, J. Gao, X. He, M. Mitchell, J. Platt, et al. From captions to visual concepts and back. In *Proc. IEEE Conf. Comp. Vis. Patt. Recogn.*, 2015.
- [14] A. Farhadi, I. Endres, D. Hoiem, and D. Forsyth. Describing objects by their attributes. In *Proc. IEEE Conf. Comp. Vis. Patt. Recogn.*, 2009.
- [15] A. Farhadi, M. Hejrati, M. A. Sadeghi, P. Young, C. Rashtchian, J. Hockenmaier, and D. Forsyth. Every picture tells a story: Generating sentences from images. In *Proc. Eur. Conf. Comp. Vis.* 2010.
- [16] H. Gao, J. Mao, J. Zhou, Z. Huang, L. Wang, and W. Xu. Are You Talking to a Machine? Dataset and Methods for Multilingual Image Question Answering. In *Proc. Adv. Neural Inf. Process. Syst.*, 2015.
- [17] X. Glorot and Y. Bengio. Understanding the difficulty of training deep feedforward neural networks. In *Proc. International Conf. Artificial Intelligence and Statistics*, pages 249–256, 2010.
- [18] Y. Gong, L. Wang, M. Hodosh, J. Hockenmaier, and S. Lazebnik. Improving image-sentence embeddings using large weakly annotated photo collections. In *Proc. Eur. Conf. Comp. Vis.* 2014.
- [19] S. Hochreiter and J. Schmidhuber. Long short-term memory. *Neural computation*, 9(8):1735–1780, 1997.
- [20] M. Hodosh, P. Young, and J. Hockenmaier. Framing image description as a ranking task: Data, models and evaluation metrics. *J. Artificial Intelligence Res.*, pages 853–899, 2013.
- [21] X. Jia, E. Gavves, B. Fernando, and T. Tuytelaars. Guiding Long-Short Term Memory for Image Caption Generation. In *Proc. IEEE Int. Conf. Comp. Vis.*, 2015.
- [22] Y. Jia, M. Salzmann, and T. Darrell. Learning cross-modality similarity for multinomial data. In *Proc. IEEE Int. Conf. Comp. Vis.*, 2011.
- [23] Y. Jia, E. Shelhamer, J. Donahue, S. Karayev, J. Long, R. Girshick, S. Guadarrama, and T. Darrell. Caffe: Convolutional Architecture for Fast Feature Embedding. *arXiv:1408.5093*, 2014.
- [24] J. Jin, K. Fu, R. Cui, F. Sha, and C. Zhang. Aligning where to see and what to tell: image caption with region-based attention and scene factorization. *arXiv:1506.06272*, 2015.
- [25] A. Karpathy and L. Fei-Fei. Deep visual-semantic alignments for generating image descriptions. In *Proc. IEEE Conf. Comp. Vis. Patt. Recogn.*, 2015.
- [26] A. Karpathy, A. Joulin, and F. F. Li. Deep fragment embeddings for bidirectional image sentence mapping. In *Proc. Adv. Neural Inf. Process. Syst.*, 2014.

- [27] R. Kiros, R. Salakhutdinov, and R. S. Zemel. Unifying visual-semantic embeddings with multimodal neural language models. In *ACM Trans. of the Association for Computational Linguistics*, 2015.
- [28] A. Krizhevsky, I. Sutskever, and G. E. Hinton. Imagenet classification with deep convolutional neural networks. In *Proc. Adv. Neural Inf. Process. Syst.*, 2012.
- [29] G. Kulkarni, V. Premraj, V. Ordonez, S. Dhar, S. Li, Y. Choi, A. C. Berg, and T. L. Berg. Babytalk: Understanding and generating simple image descriptions. *IEEE Trans. Pattern Anal. Mach. Intell.*, 35(12):2891–2903, 2013.
- [30] P. Kuznetsova, V. Ordonez, A. C. Berg, T. L. Berg, and Y. Choi. Collective generation of natural image descriptions. In *ACM Trans. of the Association for Computational Linguistics*, 2012.
- [31] P. Kuznetsova, V. Ordonez, T. L. Berg, and Y. Choi. Treetalk: Composition and compression of trees for image descriptions. *ACM Trans. of the Association for Computational Linguistics*, 2014.
- [32] C. H. Lampert, H. Nickisch, and S. Harmeling. Learning to detect unseen object classes by between-class attribute transfer. In *Proc. IEEE Conf. Comp. Vis. Patt. Recogn.*, 2009.
- [33] C. H. Lampert, H. Nickisch, and S. Harmeling. Attribute-based classification for zero-shot visual object categorization. *IEEE Trans. Pattern Anal. Mach. Intell.*, 36(3):453–465, 2014.
- [34] Y. LeCun, L. Bottou, Y. Bengio, and P. Haffner. Gradient-based learning applied to document recognition. *Proceedings of the IEEE*, 86(11):2278–2324, 1998.
- [35] L.-J. Li, H. Su, L. Fei-Fei, and E. P. Xing. Object bank: A high-level image representation for scene classification & semantic feature sparsification. In *Proc. Adv. Neural Inf. Process. Syst.*, pages 1378–1386, 2010.
- [36] L.-J. Li, H. Su, Y. Lim, and L. Fei-Fei. Objects as attributes for scene classification. In *Trends and Topics in Computer Vision*, pages 57–69. Springer, 2012.
- [37] S. Li, G. Kulkarni, T. L. Berg, A. C. Berg, and Y. Choi. Composing simple image descriptions using web-scale n-grams. In *Proc. SIGNLL Conf. Computational Natural Language Learning*, 2011.
- [38] T.-Y. Lin, M. Maire, S. Belongie, J. Hays, P. Perona, D. Ramanan, P. Dollár, and C. L. Zitnick. Microsoft COCO: Common objects in context. In *Proc. Eur. Conf. Comp. Vis.* 2014.
- [39] L. Ma, Z. Lu, and H. Li. Learning to Answer Questions From Image using Convolutional Neural Network. *arXiv:1506.00333*, 2015.
- [40] M. Malinowski and M. Fritz. A multi-world approach to question answering about real-world scenes based on uncertain input. In *Proc. Adv. Neural Inf. Process. Syst.*, pages 1682–1690, 2014.
- [41] M. Malinowski and M. Fritz. Hard to Cheat: A Turing Test based on Answering Questions about Images. *arXiv:1501.03302*, 2015.
- [42] M. Malinowski, M. Rohrbach, and M. Fritz. Ask Your Neurons: A Neural-based Approach to Answering Questions about Images. In *Proc. IEEE Int. Conf. Comp. Vis.*, 2015.
- [43] J. Mao, W. Xu, Y. Yang, J. Wang, and A. Yuille. Deep Captioning with Multimodal Recurrent Neural Networks (m-RNN). In *Proc. Int. Conf. Learning Representations*, 2015.
- [44] T. Mikolov, I. Sutskever, K. Chen, G. S. Corrado, and J. Dean. Distributed representations of words and phrases and their compositionality. In *Proc. Adv. Neural Inf. Process. Syst.*, pages 3111–3119, 2013.
- [45] G. A. Miller. WordNet: a lexical database for English. *Communications of the ACM*, 38(11):39–41, 1995.
- [46] M. Mitchell, X. Han, J. Dodge, A. Mensch, A. Goyal, A. Berg, K. Yamaguchi, T. Berg, K. Stratos, and H. Daumé III. Midge: Generating image descriptions from computer vision detections. In *Proc. Conf. of the European Chapter of the Association for Computational Linguistics*, 2012.
- [47] V. Ordonez, G. Kulkarni, and T. L. Berg. Im2text: Describing images using 1 million captioned photographs. In *Proc. Adv. Neural Inf. Process. Syst.*, 2011.
- [48] K. Papineni, S. Roukos, T. Ward, and W.-J. Zhu. BLEU: a method for automatic evaluation of machine translation. In *ACM Trans. of the Association for Computational Linguistics*, 2002.
- [49] J. Pont-Tuset, P. Arbeláez, J. Barron, F. Marques, and J. Malik. Multiscale Combinatorial Grouping for Image Segmentation and Object Proposal Generation. In *arXiv:1503.00848*, March 2015.
- [50] M. Ren, R. Kiros, and R. Zemel. Image Question Answering: A Visual Semantic Embedding Model and a New Dataset. In *Proc. Adv. Neural Inf. Process. Syst.*, 2015.
- [51] M. Rohrbach, W. Qiu, I. Titov, S. Thater, M. Pinkal, and B. Schiele. Translating video content to natural language descriptions. In *Proc. IEEE Int. Conf. Comp. Vis.*, 2013.
- [52] K. Simonyan and A. Zisserman. Very deep convolutional networks for large-scale image recognition. *arXiv:1409.1556*, 2014.
- [53] R. Socher, A. Karpathy, Q. V. Le, C. D. Manning, and A. Y. Ng. Grounded compositional semantics for finding and describing images with sentences. *ACM Trans. of the Association for Computational Linguistics*, 2014.
- [54] Y. Su and F. Jurie. Improving image classification using semantic attributes. *Int. J. Comp. Vis.*, 100(1):59–77, 2012.

- [55] I. Sutskever, O. Vinyals, and Q. V. Le. Sequence to sequence learning with neural networks. In *Proc. Adv. Neural Inf. Process. Syst.*, 2014.
- [56] C. Szegedy, W. Liu, Y. Jia, P. Sermanet, S. Reed, D. Anguelov, D. Erhan, V. Vanhoucke, and A. Rabinovich. Going deeper with convolutions. In *Proc. IEEE Conf. Comp. Vis. Patt. Recogn.*, 2015.
- [57] R. Vedantam, C. L. Zitnick, and D. Parikh. CIDEr: Consensus-based Image Description Evaluation. In *Proc. IEEE Conf. Comp. Vis. Patt. Recogn.*, 2015.
- [58] O. Vinyals, A. Toshev, S. Bengio, and D. Erhan. Show and tell: A neural image caption generator. In *Proc. IEEE Conf. Comp. Vis. Patt. Recogn.*, 2014.
- [59] J. Vogel and B. Schiele. Semantic modeling of natural scenes for content-based image retrieval. *Int. J. Comp. Vis.*, 72(2):133–157, 2007.
- [60] Y. Wei, W. Xia, J. Huang, B. Ni, J. Dong, Y. Zhao, and S. Yan. CNN: Single-label to multi-label. *arXiv:1406.5726*, 2014.
- [61] Z. Wu and M. Palmer. Verbs semantics and lexical selection. In *ACM Trans. of the Association for Computational Linguistics*, 1994.
- [62] K. Xu, J. Ba, R. Kiros, A. Courville, R. Salakhutdinov, R. Zemel, and Y. Bengio. Show, Attend and Tell: Neural Image Caption Generation with Visual Attention. In *Proc. Int. Conf. Mach. Learn.*, 2015.
- [63] Y. Yang, C. L. Teo, H. Daumé III, and Y. Aloimonos. Corpus-guided sentence generation of natural images. In *Proc. Conf. Empirical Methods on Natural Language Processing*, 2011.
- [64] P. Young, A. Lai, M. Hodosh, and J. Hockenmaier. From image descriptions to visual denotations: New similarity metrics for semantic inference over event descriptions. *ACM Trans. of the Association for Computational Linguistics*, 2, 2014.
- [65] C. Zhang, J. C. Platt, and P. A. Viola. Multiple instance boosting for object detection. In *Proc. Adv. Neural Inf. Process. Syst.*, 2005.
- [66] Y. Zhu, C. Zhang, C. Ré, and L. Fei-Fei. Building a Large-scale Multimodal Knowledge Base for Visual Question Answering. *arXiv:1507.05670*, 2015.